

1
2
3
4 **BIOMASS GASIFICATION CHARs FOR**
5 **MERCURY CAPTURE FROM A SIMULATED**
6 **FLUE GAS OF COAL COMBUSTION**
7
8
9
10

11 A. Fuente-Cuesta¹, M. Diaz-Somoano¹, M.A. Lopez-Anton^{1*}, M. Cieplik², J.L.G.
12 Fierro³, M.R. Martínez-Tarazona¹
13
14

15 ¹Instituto Nacional del Carbón (CSIC). C/ Francisco Pintado Fe N° 26, 33011, Oviedo,
16 Spain
17

18 ²Energy Research Centre of the Netherlands, Biomass, P.O. Box 1, Petten, 1755 ZG,
19 Netherlands
20

21 ³Instituto de Catálisis y Petroleoquímica (CSIC), C/Marie Curie 2, Campus de
22 Cantoblanco, 28049-Madrid, Spain
23
24
25
26
27
28
29
30

31 **Corresponding author*
32 Phone: +34 985119090
33 Fax: +34 985297662
34 e-mail: marian@incar.csic.es
35
36
37
38
39

40
41
42
43

Abstract

44 The combustion of coal can result in trace elements, such as mercury, being released
45 from power stations with potentially harmful effects for both human health and the
46 environment. Research is ongoing to develop cost-effective and efficient control
47 technologies for mercury removal from coal-fired power plants, the largest source of
48 anthropogenic mercury emissions. A number of activated carbon sorbents have been
49 demonstrated to be effective for mercury retention in coal combustion power plants.
50 However, more economic alternatives need to be developed. Raw biomass gasification
51 chars could serve as low-cost sorbents for capturing mercury since they are sub-
52 products generated during a thermal conversion process. The aim of this study was to
53 evaluate different biomass gasification chars as mercury sorbents in a simulated coal
54 combustion flue gas. The results were compared with those obtained using a
55 commercial activated carbon. Chars from a mixture of paper and plastic waste showed
56 the highest retention capacity. It was found that not only a high carbon content and a
57 well developed microporosity but also a high chlorine content and a high aluminium
58 content improved the mercury retention capacity of biomass gasification chars. No
59 relationship could be inferred between the surface oxygen functional groups and
60 mercury retention in the char samples evaluated.

61

62 **Keywords:** mercury; coal combustion; char; biomass

63

64

65

66

67 **1. Introduction**

68
69 Coal combustion is a significant, if not the main, source of mercury emissions in
70 many countries. Different technologies and policies (EC, 2005; Milford and Pienciak,
71 2009; Pacyna et al., 2010; UNEP, 2010; USEPA, 2011) have been proposed during the
72 last two decades to control these emissions. The leading technology is the injection of
73 powdered activated carbon into the flue gas, prior to the particulate control devices
74 (PCD). In some cases, the activated carbon may be injected after the PCD and collected
75 in a separate or secondary downstream PCD (Sjostrom et al., 2010). However, further
76 advances in this field are still necessary to reduce costs and limit the balance-of-plant
77 impacts associated with the use of the activated carbons (Pflughoeft-Hassett et al., 2009;
78 Sjostrom et al., 2010). In other words, there is a clear need to develop new and cheaper
79 mercury sorbents that can replace the expensive materials used at the moment.

80 Gasification has emerged as a clean and effective way to produce gas from
81 biomass and is considered a promising technology for producing chemicals and energy
82 from renewable sources. Char is the finest component of the gasifier slag. The high
83 carbonaceous matter content and the presence of relevant elements such as sulphur and
84 chlorine in chars make them good potential sorbents for mercury species. Gasification
85 char is a “waste,” and therefore, significantly less expensive than a manufactured
86 sorbent.

87 Several coal chars have already been tested in a variety of conditions for
88 mercury adsorption. A number of chars from bituminous and sub-bituminous coals have
89 been used in simulated flue gas at 160 °C to show the importance of the coal rank in
90 mercury capture (Wu et al., 2000). Maroto-Valer et al. (2004) compared the mercury
91 retention capacity of a high carbon char with a commercial activated carbon in a fixed
92 bed at 138 °C and found that the surface functionality of chars played an important role

93 in mercury retention while their surface area did not seem to have any significant impact
94 on mercury retention capacity. Chars from the Integrated Gasification Combined-Cycle
95 (IGCC) were injected in a lab-scale plant to evaluate the amount of mercury captured
96 (Cao et al., 2004). The results showed a high mercury retention efficiency at a low
97 temperature (20 °C) and a short residence time (0.13 s) (Cao et al., 2004). In a project
98 developed in conjunction with the University of Kentucky Center for Applied Energy
99 Research (CAER), the use of combustion and gasifier by-products as sorbents for
100 mercury and NO_x adsorption was studied and compared to commercial activated
101 carbons designed specifically for the capture of these elements (Rubel et al., 2004).
102 Mercury sorption testing was performed using a fixed bed reactor. Combustion by-
103 products were found to adsorb very little mercury and NO_x, whereas an untreated
104 gasifier char carbon was observed to adsorb as much mercury as the commercial
105 activated carbon. Moreover, NO_x adsorption was slightly improved by the gasifier by-
106 product which was heavily laden with mercury indicating different adsorption
107 mechanisms and/or sites for mercury and NO_x adsorption. Thus, this material, even if
108 its primary function is mercury removal from flue gas, could also potentially be used to
109 reduce NO_x emissions (Rubel et al., 2004). Not having to subject the char to pre-
110 treatment is another significant benefit, as additional costs can thereby be avoided.
111 Although previous studies have used activated chars from biomass to remove mercury
112 from the simulated flue gas of coal combustion (Klasson et al., 2010), there is still a
113 lack of knowledge concerning the behaviour of untreated biomass chars as mercury
114 sorbents. The ultimate objective of this work is to develop low-cost sorbents for direct
115 injection into power plants. For this purpose, a preliminary study at lab-scale was
116 carried out using raw gasification chars from different biomasses to evaluate their
117 mercury adsorption capacity in relation to their properties.

118

119 **2. Experimental**

120 Eight biomass gasification chars from agricultural sources, poultry litter and
121 wood, and one activated carbon were tested as mercury sorbents. The char called SH is
122 the sub-product of the gasification of sunflower husks, while the one denoted PL is from
123 poultry litter. The other six chars were: one from clean wood pellets (CW), two from
124 wood waste (WW1, WW2) and three from a mixture of paper and plastic waste (PW1,
125 PW2, PW3). The activated carbon is a commercial activated carbon impregnated with
126 sulphur (Filtracarb D47/7+S). The chars were obtained from a pilot gasification plant of
127 500 kW with a circulated fluidized bed (CFB) gasifier BIVKIN in the Energy Research
128 Centre of the Netherlands (ECN).

129 These materials were characterized by various methods before being used as
130 sorbents. The hydrogen, nitrogen and sulphur contents were determined by LECO
131 automatic analyzers, whereas the total carbon (TC), total organic carbon (TOC) and
132 inorganic carbon (IC) contents were determined using a TOC V-CPH E200V device.
133 The oxygen content was calculated by difference with the elements just mentioned,
134 bearing in mind the errors inherent in this procedure. X-ray fluorescence (XRF) was
135 used to determine the composition of the major elements. The chlorine content was
136 determined by ionic chromatography. The unburned carbon particle content in each char
137 was estimated as loss of ignition (LOI) by combustion of the organic matter at 815 °C.
138 The porous texture of the gasification chars and the activated carbon was determined by
139 N₂ and CO₂ adsorption isotherms at -196 °C and 0 °C, respectively. The crystalline
140 species in the mineral matter of the chars and the activated carbon obtained by Low
141 Temperature Ashing (LTA) were identified by X-ray diffraction (XRD). The mode of
142 occurrence of sulphur in the sorbents was analyzed by X-ray photoemission

143 spectroscopy (XPS). XP spectra were obtained with a VG Escalab 200R spectrometer
144 equipped with a hemispherical electron analyser and a MgK α ($h\nu = 1254.6$ eV) X-ray
145 source. The kinetic energies of photoelectrons were measured using a hemispherical
146 electron analyser working in the constant pass energy mode. Binding energies were
147 calibrated relative to the C 1s peak at 284.9 eV. High resolution spectra envelopes were
148 obtained by curve fitting synthetic peak components using the software “*XPS peak*”.
149 The surface oxygen groups were identified by temperature-programmed desorption
150 (TPD) using an Autochem II analyzer coupled to an OmnistarTM mass detector in argon
151 atmosphere. The pH of the chars was measured according to the following procedure:
152 40 mg of sample was added to 2 mL of water and the suspension was stirred during 48 h
153 to reach equilibrium. Then, the pH of solution was measured.

154 The experimental device used for retention consisted of a glass reactor fitted to
155 an internal and external tube and heated in a furnace (Figure 1). The sorbent was placed
156 inside the internal tube. The sorbent bed was prepared by mixing 20 mg of char or
157 activated carbon with 60 mg of sand. The temperature of the sorbent bed was kept at
158 150 °C. Elemental mercury in gas phase was obtained from a permeation tube. A
159 synthetic gas mixture containing the species present in the coal combustion atmosphere
160 (5% O₂, 1300 mg Nm⁻³ SO₂, 500 mg Nm⁻³ NO₂, 20.3 mg Nm⁻³ HCl) was passed through
161 the reactor. This gas mixture carried the mercury in vapour phase through the sorbent
162 bed at a flow rate of 0.5 L min⁻¹. The mercury concentration in gas phase was
163 approximately 100 $\mu\text{g m}^{-3}$. The duration of the mercury retention experiments varied
164 depending on the type of char but in general it was the time needed for the samples to
165 reach their maximum retention capacity. The mercury not retained in the sorbents was
166 measured using a continuous mercury monitor (VM-3000). The mercury content before

167 and after the retention experiments was determined by means of an automatic mercury
168 analyzer (AMA).

169 **3. Results and discussion**

170 The proximate and elemental analysis and inorganic composition of the chars
171 and the activated carbon are shown in Table 1. It can be seen that the gasification chars
172 employed in this study display different characteristics, allowing us to evaluate the main
173 parameters that affect mercury retention. The ash content ranges from 22% for the char
174 from the sunflower husks (SH) to 75% for poultry litter (PL) and paper-plastic waste
175 (PW3) (thus the loss-on-ignition (LOI) values are between 78 and 25%). The volatile
176 matter content ranges between 7-10% for all the chars with the exception of SH and the
177 char from clean wood (CW), in both of which it reaches values of 22%. Apart from the
178 carbonaceous material which is the active sorbent, the mineral components as a medium
179 of mercury capture or as a catalyst in the sorption process also need to be considered.
180 Therefore, the following differences in composition must be pointed out: (i), the high
181 potassium content found in the SH char; (ii), the high potassium, sodium, calcium,
182 magnesium and phosphorus contents in PL; and (iii), the high amount of silicon and
183 aluminium in the CW and PW chars, respectively (Table 1). Also, since it is well known
184 that mercury species may react with sulphur and chlorine (Yang et al., 2007) special
185 attention needs to be paid to the content of these two elements in the different samples
186 studied. With respect to sulphur content and mode of occurrence, the CW and PW chars
187 were found to contain the smallest quantity (0.02-0.1% wt), whereas SH, WW and PL
188 contained approximately 0.5, 0.8 and 1.7% (wt), respectively. The sulphur content of
189 the commercial activated carbon was 2.5% (Table 1). The different modes of occurrence
190 of sulphur in the samples were revealed by means of XPS. The binding energies of the

191 S2p core-level spectra displayed in Figure 2 indicate the occurrence of one or two peaks
192 components located at about 164.7 eV and or 168.9 eV belonging to elemental/organic
193 ($S^0/C-S$) sulphur and sulphate (S^{6+}) species, respectively. It was observed that the
194 relative proportions of S^{6+} and other forms of sulphur, indistinguishable by XPS ($S^0/C-$
195 S), were in fact different in each of the samples. In the Filtracarb activated carbon the
196 proportion of $S^0/C-S$ was the most prominent, while in the char samples either it was
197 not identified or it was present in very low proportions. The char obtained from the
198 wood waste presented similar proportions for both forms of sulphur (Figure 2). As
199 regards chlorine content, the PW chars showed the highest values (5-6%), while SH, PL
200 and WW contained approximately 0.8, 1.8 and 3%, respectively. The CW char and
201 Filtracarb activated carbon were found to contain only a small quantity of chloride
202 (Table 1).

203 The crystalline phases, as estimated by XRD, were mainly calcite ($CaCO_3$) and
204 quartz (SiO_2) in all the char samples with the exception of the char from clean wood in
205 which quartz was the only mineral identified. In SH and PL dolomite ($CaMg(CO_3)_2$)
206 and silvite (KCl) were also found, while in the samples from wood waste (WW1-2),
207 rutile (TiO_2) was present. Metallic aluminium was also found in the chars from the
208 plastic-paper waste. The minerals detected in the activated carbon were mainly silica
209 oxides (quartz) and hematite (Fe_2O_3).

210 The porous textural characteristics of the biomass chars and the activated carbon
211 were studied comparatively using adsorption-desorption isotherms of N_2 and CO_2 . The
212 N_2 adsorption isotherm for Filtracarb belonged to type I in the BDDT classification
213 (typical of microporous solids) with only a minor participation from type IV. These had
214 a narrow type H4 hysteresis loop, indicating the occurrence of slit-shaped mesopores.
215 The N_2 adsorption isotherms for the biomass chars were somewhere between type I and

216 type IV. The values for the surface area, total pore volume, micropore volume by fitting
217 the Dubinin-Radushkevich (DR) and the mesopore volume in the activated carbon and
218 chars are given in Table 2. The N₂ adsorption isotherms for the activated carbon yielded
219 a BET surface area value of 560 m²g⁻¹, while in the char samples the BET values
220 ranged from 2 to 65 m²g⁻¹. The highest surface area values corresponded to the chars
221 from the plastic-paper waste (Table 2). The CO₂ adsorption isotherms were performed
222 in the relative pressure interval of 0-0.03, where only the narrowest micropores were
223 filled. The results for micropore volume obtained by fitting the Dubinin-Radushkevich
224 (DR) equation to the CO₂ adsorption isotherms at 0 °C are shown in Table 2. The
225 micropore volume obtained from DR for CO₂ was lower than that of N₂ in the activated
226 carbon. This activated carbon has a well developed microporosity with pores in which
227 the CO₂ is unable to fill. However, in the char samples the micropore volume for CO₂
228 was higher than the micropore volume for N₂ (Table 2). Therefore, these biomass chars
229 present a very narrow microporosity, of the order of ultra-micropores.

230 Previous studies have suggested that oxygen functional groups, such as,
231 carboxyl, lactone, phenolic, carbonyl, have an impact on elemental mercury adsorption
232 on carbonaceous surface sites (Li et al., 2002; Liu et al., 2011; Skodras et al., 2007). In
233 this study, the surface functional groups were characterized by TPD (Figures 3-4).
234 Although there is some controversy as to the assignment of TPD peaks to specific
235 surface groups, some general trends have been established (Figueiredo et al., 1999;
236 Szymanski et al., 2002). The main oxygen groups identified in the Filtracarb activated
237 carbon are carboxylic anhydrides with both CO and CO₂ peaks at approximately 650 °C.
238 The greater intensity of the CO peak compared to the CO₂ peak also suggests the
239 presence of phenols/ethers (Figure 3). Comparing the spectra of the activated carbon to
240 with those of the char samples (Figure 4), we observe: (i), a very small amount of

241 surface oxygen groups in the char samples which is evidenced by the decrease in the
242 CO and CO₂ peaks, (see the scale of the y-axis), especially in the chars from the plastic-
243 paper waste; (ii), the lack of parallelism between the peaks of CO and CO₂; and (iii), the
244 narrow peaks present in the CO₂ TPD profile in some of the samples possibly due to the
245 decomposition of calcium compounds. With the exception of the CW char, the samples
246 have an inorganic carbon content between 1-2% and a calcium content between 4-17%
247 (Table 1). Moreover, calcite was identified by DRX. It should also be noted that some
248 chars may have been pyrolyzed at temperature higher than 600 °C (Figure 4).

249 The pH of the char and activated carbon suspensions was also measured to
250 determine the acidity and basicity of the surface of the sorbents and its possible
251 influence on the retention of mercury. The pH value for the activated carbon was 5.8
252 whereas for the char samples it ranged from 7.6 to 11.4, the lowest pH corresponding to
253 the chars from the plastic-paper waste.

254 The mercury content before and after the retention experiments is presented in
255 Table 3. The confidence limit of the results represented by the relative standard
256 deviation is <15 %. The samples were employed in sizes as received. The size of the
257 chars ranged from approximately 29 to 58 μm with the exception of the CW char (136
258 μm). The mercury retention capacity in the char samples could be arranged in
259 increasing order as PW > SH > PL ~ WW > CW (Table 3). It should be pointed out that
260 some PW chars which had a much lower surface area than the activated carbon
261 achieved similar mercury retentions (~200 μg g⁻¹) (Tables 2-3).

262 In general, no relationship was found between mercury retention and the
263 inorganic components of the chars presented in Table 1. Nevertheless, we must
264 emphasize that a higher mercury capture was observed in the group of samples with a
265 high aluminum and chlorine content (Figure 5), the SH char being the exception in both

266 cases. Although the presence of sulfur is bound to influence the retention of mercury, no
267 relation was observed between mercury retention capacity and sulphur content of the
268 char samples. This is due to not only to the amount of sulphur but also its mode of
269 occurrence in the sorbents. In fact, according to the XPS analysis, the form of sulphur
270 identified mainly in the Filtracarb activated carbon was S^0 or organic sulphur (probably
271 S^0 , which would favour chemical reaction with elemental mercury) while sulphate was
272 the main form identified in most of the char samples (Figure 2).

273 Although the char samples are solids with a low surface area (Table 2), and their
274 values are obviously not as significant as those of the activated carbons, in general the
275 increasing surface area of the char samples would enhance mercury capture (Figure 6a).
276 However, the SH char which did not have high surface area values, or, as already
277 mentioned, a high chlorine content (Figure 5) showed a high mercury retention capacity.
278 Other parameters therefore, must be taken into account. The SH char had a high narrow
279 micropore volume content for CO_2 , similar to that of the activated carbon content (Table
280 2). It also exhibited the highest carbon content (LOI) (Table 1). Figure 6b shows the
281 LOI content versus the mercury retention capacity for the char samples. When all char
282 samples are compared the relation is clearly not linear. However, a close examination of
283 the retention by each group of chars from the same type of biomass (plastic-paper or
284 wood) shows that retention increased when the LOI increased (Figure 6b). A similar
285 relationship to that of LOI and mercury retention was observed for total carbon (TC)
286 and total organic carbon (TOC) content (Table 1). To sum up, the results show that
287 mercury retention is improved by a high chlorine content and high surface area and high
288 narrow micropore volume values and that the carbon content also play an important role
289 in mercury capture. A high aluminum content may also favor mercury retention. It

290 should also be noted that, in general, chars such as PW1-3 with a neutral pH (~7-8)
291 show a higher retention capacity than those with basic pH (~10-11).

292 With respect to the role of the surface functional groups in mercury capture,
293 from the results obtained with the Filtracarb activated carbon, it can be inferred that the
294 textural properties (Table 2) and the mode of occurrence of sulphur (Figure 2) are
295 important for mercury retention with oxygenated groups, mainly acid groups as
296 demonstrated from TPD results (Figure 3), and pH value (5.8) also playing an important
297 role. However, in solids such as the char samples which have a large amount of mineral
298 matter (22-75% ash content) and in which the decomposition of organic matter resulting
299 from the high temperatures (1000 °C) cannot be ruled out, no clear relationship between
300 mercury capture and surface oxygen groups could be established. Moreover, as can be
301 seen in Figure 4, the chars from the plastic-paper waste have the smallest amount of
302 surface oxygen groups and yet these samples displayed the greatest mercury retention
303 capacity (Table 3).

304

305 **4. Conclusion**

306 Although untreated chars do not have as much surface area or sulphur content as
307 commercial activated carbon, some chars resulting from biomass gasification, mainly
308 from plastic-paper waste, showed high mercury retention capacities in the simulated
309 flue gas of coal combustion. Therefore, these low-cost sorbents could serve as an
310 attractive alternative to activated carbons for direct injection into power plants. Apart
311 from the advantages of a high carbon content and good textural characteristics, mercury
312 retention in the char samples was found to be favoured by a high chloride content and a
313 low pH. No relation was found between mercury retention and surface chemistry.

314

315

316

317 **Acknowledgments**

318

319 The financial support for this work was provided by the project MERCURYCAP
320 (RFCR-CT-2007-00007). The authors thank the Energy Research Centre of the
321 Netherlands for supplying the chars employed in this study and the Spanish Research
322 Council (CSIC) for awarding Ms. Aida Fuente-Cuesta a pre-doctoral fellowship.

323

324

325 **References**

326 Cao, Y., Liu, K., Liu, X., Yang, H., Riley, J.T., Pan, W-P., 2004. The lab-scale sorbent
327 injection testing on mercury capture with follow-up solid-gas mixture. Prepr. Pap.-
328 Am. Chem. Soc., Div. Fuel Chem. 49(2), 918-919.

329 EC. Communication from the Commission of the European Communities to the Council
330 and the European Parliament- Community Strategy Concerning Mercury. {SEC
331 (2205) 101}, 2005; [http://eur-lex.europa.eu/LexUriServ/LexUriServ.do?uri=COM:
332 2005:0020:FIN:EN:PDF](http://eur-lex.europa.eu/LexUriServ/LexUriServ.do?uri=COM:2005:0020:FIN:EN:PDF).

333 Figueiredo, J.L., Pereira, M.F.R., Freitas, M.M.A., Orfao, J.J.M., 1999. Modification of
334 the surface chemistry of activated carbons. Carbon 37, 1379-1389.

335 Klasson, K.T., Lima, I.M., Boihem Jr, L.L., Wartelle, L.H., 2010. Feasibility of mercury
336 removal from simulated flue gas by activated chars made from poultry manures. J.
337 Environ. Manage. 91, 2466-2470.

338 Li, Y.H., Lee, C.W., Gullett, B.K., 2002. The effect of activated carbon surface
339 moisture on low temperature mercury adsorption. Carbon 40, 65-72.

340 Liu, J., Cheney, M.A., Wu, F., Li, M., 2011. Effects of chemical functional groups on
341 elemental mercury adsorption on carbonaceous surfaces. *J. Hazard. Mater.* 186, 108-
342 113.

343 Maroto-Valer, M.M., Zhang, Y., Miller, B.G., Granite, E., Tang, Z., Pennline, H., 2004.
344 Mercury oxidation and capture by coal chars. Available in:
345 http://acs.omnibooksonline.com/data/papers/2004_L035.pdf

346 Milford, J.B., Pienciak, A., 2009. After the Clean Air Mercury Rule: Prospects for
347 reducing mercury emissions from coal-fired power plants. *Environ. Sci. Technol.*
348 43(8), 2669-2673.

349 Pacyna, J., Sundseth, K., Pacyna, E.G., Jozewicz, W., Munthe, J., Belhaj, M., Astrom,
350 S., 2010. An Assessment of Costs and Benefits Associated with Mercury Emission
351 Reductions from Major Anthropogenic Sources. *J. Air Waste Manage.* 60, 302-315.

352 Pflughoeft-Hassett, D.F., Hassett, D.J., Buckley, T.D., Heebink, L.V., Pavlish, J.H.,
353 2009. Activated carbon for mercury control: Implications for fly ash management.
354 *Fuel Process. Technol.* 90, 1430-1434.

355 Rubel, A.M., Andrews, R., Gonzalez, R., Groppo, J., Robl, T., 2004. Mercury
356 adsorption on combustion and gasifier by-products. Presented in the 56th Southeast
357 Regional Meeting of the American Chemistry Society, November 10-13, 2004.
358 Research Triangle Park, North Carolina, USA.

359 Sjostrom, S., Durham, M., Bustard, C.J., Martin, C., 2010. Activated carbon injection
360 for mercury control: Overview. *Fuel* 89, 1320-1322.

361 Skodras, G., Diamantopoulou, Ir., Zabaniotou, A., Stavropoulos, G., Sakellaropoulos,
362 G.P., 2007. Enhance mercury adsorption in activated carbons from biomass
363 materials and waste tires. *Fuel Process. Technol.* 88, 749-758.

364 Szymanski, G.S., Karpinski, Z., Biniak, S., Swiatkowski, A., 2002. The effect of the
365 gradual thermal decomposition of surface oxygen species on the chemical and
366 catalytic properties of oxidized activated carbon. Carbon 40, 2627-2639.

367 UNEP. United Nations Environment Programme. Process Optimization Guidance
368 Document for Reducing Mercury Emissions from Coal Combustion in Power
369 Plants, Chemical Branch, DTIE, Geneva, Switzerland, Draft report, July 2010.

370 USEPA. United States Environmental Protection Agency. National Emission Standards
371 for Hazardous Air Pollutants from Coal- and Oil-fired Electric Utility Steam
372 Generating Units and Standards of Performance for Fossil-Fuel-Fired Electric
373 Utility, Industrial-Commercial-Institutional, and Small Industrial-Commercial-
374 Institutional Steam Generating Units. 2011; [http://www.epa.gov/airquality/
375 powerplanttoxics/pdfs/proposal.pdf](http://www.epa.gov/airquality/powerplanttoxics/pdfs/proposal.pdf)

376 Wu, B., Peterson, T.W., Shadman, F., Senior, C.L., Morency, J.R., Huggins, F.E.,
377 Huffman, G.P., 2000. Interactions between vapour-phase mercury compounds and
378 coal char in synthetic flue gas. Fuel Process. Technol. 63, 93-107.

379 Yang, H., Xu, Z., Fan, M., Bland, A.E., Judkins, R.R., 2007. Adsorbents for capturing
380 mercury in coal-fired boiler flue gas. J. Hazard. Mater. 146, 1-11

Table 1. Proximate and ultimate analysis and elemental composition of the inorganic components of the char samples and the activated carbon (wt% db)

	SH	PL	CW	WW1	WW2	PW1	PW2	PW3	Filtracarb
Moisture	<0.1	2.0	0.3	2.7	2.1	<0.1	0.4	1.5	4.2
Ash	21.7	74.9	53.6	45.4	48.9	45.1	55.1	75.4	14.1
Volatile matter	21.7	10.4	22.4	8.7	6.8	8.2	7.4	8.6	14.9
LOI	78.3	25.1	46.4	54.5	51.1	54.9	44.9	24.6	85.9
TC	56.8	13.6	29.1	39.6	39.4	34.3	26.2	15.8	68.3
TOC	55.0	11.7	29.1	38.6	37.8	32.7	24.6	14.2	68.3
IC	1.8	1.9	0.0	1.0	1.6	1.6	1.6	1.6	0.0
H	1.9	0.6	0.6	0.7	0.8	2.4	2.0	1.4	0.73
N	0.90	1.1	0.0	0.7	0.7	0.27	0.20	0.11	2.9
S	0.50	1.7	0.02	0.86	0.70	0.09	0.08	0.11	2.5
O	18.2	8.1	16.7	12.7	9.6	17.8	16.5	7.2	11.5
Cl	0.76	1.8	0.11	3.0	2.6	4.65	5.2	5.9	0.07
Na	0.36	2.2	0.13	0.41	0.45	0.13	0.28	0.40	0.23
K	3.7	3.1	0.51	0.26	0.82	0.04	0.03	0.26	0.39
Si	2.7	9.4	21.9	7.8	11.1	7.06	7.7	16.5	3.1
Ca	3.6	17.1	1.2	7.0	8.7	9.00	9.6	9.7	0.62
Fe	0.16	0.37	0.18	0.77	1.03	0.62	0.94	1.3	1.5
Al	0.44	0.44	0.87	2.6	1.3	7.3	10.4	9.6	2.1
Ti	0.08	0.03	0.02	1.6	2.1	1.0	1.2	1.2	0.11
Mg	1.9	2.9	0.17	0.80	0.99	0.72	0.94	0.95	0.20
P	0.93	5.5	0.03	0.20	0.17	0.08	0.10	0.12	0.04

LOI: loss of ignition; TC: total carbon; TOC: total organic carbon; IC: inorganic carbon

Table 2. Surface area, total pore volume, micropore volume by DR and mesopore volume to the N₂ adsorption and micropore volume by DR to the CO₂ adsorption in the char samples and the activated carbon

Sample	S_{BET} ($\text{m}^2 \cdot \text{g}^{-1}$)	V_t ($\text{cm}^3 \cdot \text{g}^{-1}$)	V_{mN_2} ($\text{cm}^3 \cdot \text{g}^{-1}$)	V_{meso} ($\text{cm}^3 \cdot \text{g}^{-1}$)	V_{mCO_2} ($\text{cm}^3 \cdot \text{g}^{-1}$)
SH	5	0.006	0.002	0.004	0.129
PL	12	0.013	0.005	0.008	0.027
CW	5	0.006	0.002	0.004	0.075
WW1	2	0.005	0.001	0.004	0.076
WW2	2	0.004	0.001	0.003	0.074
PW1	65	0.045	0.030	0.015	0.065
PW2	42	0.035	0.020	0.015	0.052
PW3	20	0.021	0.009	0.012	0.032
Filtracarb	560	0.293	0.236	0.057	0.153

Table 3. Mercury content in the raw char samples and the activated carbon and mercury retention capacity

Sample	Hg ($\mu\text{g} \cdot \text{g}^{-1}$)	Hg retained ($\mu\text{g} \cdot \text{g}^{-1}$)
SH	0.01	120
PL	0.02	36
CW	0.01	6.0
WW1	0.01	33
WW2	0.02	31
PW1	0.01	172
PW2	0.01	164
PW3	0.01	78
Filtracarb	0.34	227

Figure captions

Figure 1. Schematic diagram of experimental device for mercury retention

Figure 2. S2p core-level spectra of Filtracarb activated carbon and char samples

Figure 3. TDP profiles of (a) CO evolution and (b) CO₂ evolution in the activated carbon

Figure 4. TDP profiles of (a) CO evolution and (b) CO₂ evolution in the char samples

Figure 5. Chlorine content (a) and aluminium content (b) versus mercury retention capacity in the char samples

Figure 6. BET surface area (a) and unburned carbon content (LOI) (b) versus mercury retention capacity in the char samples

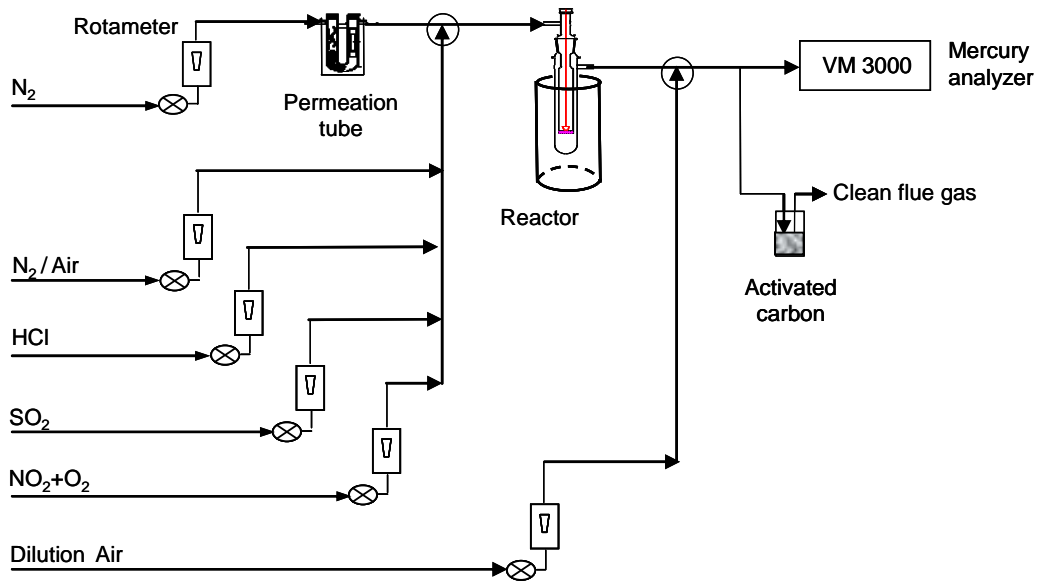


Figure 1.

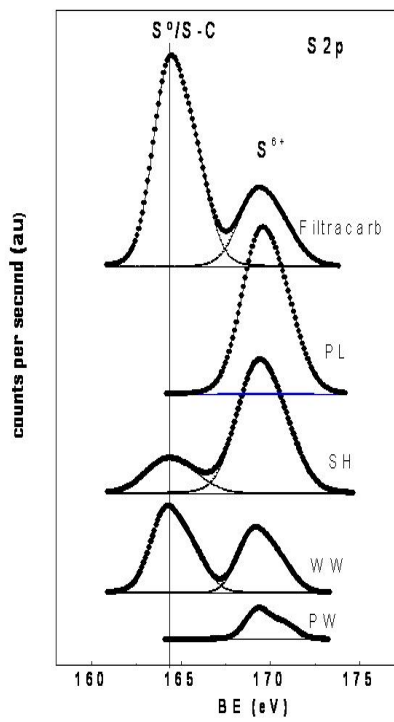
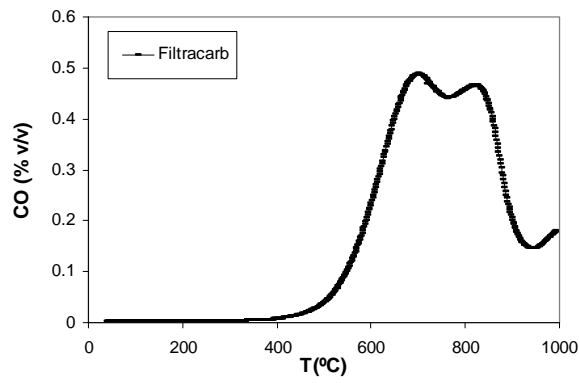
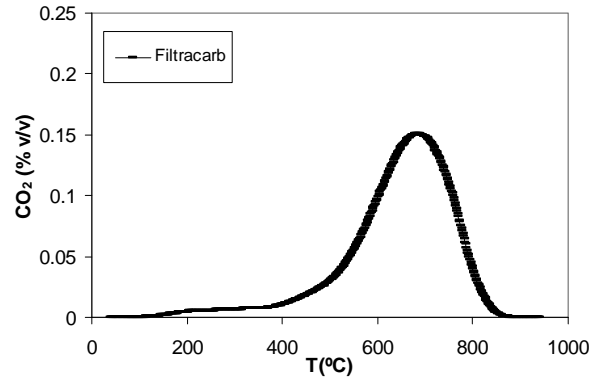


Figure 2.

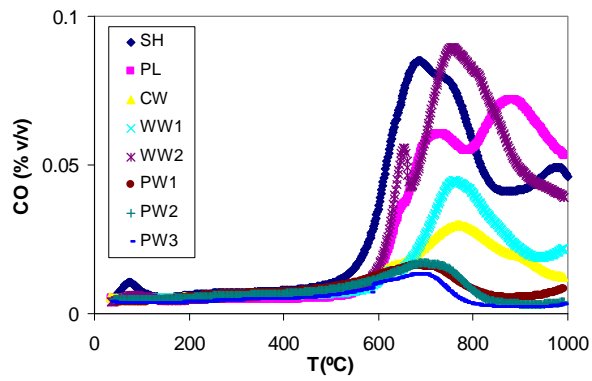


(a)

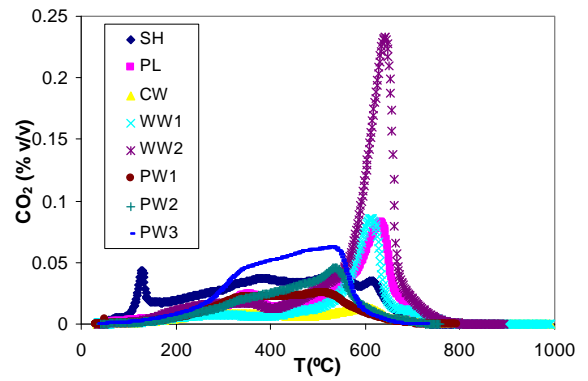


(b)

Figure 3.



(a)



(b)

Figure 4.

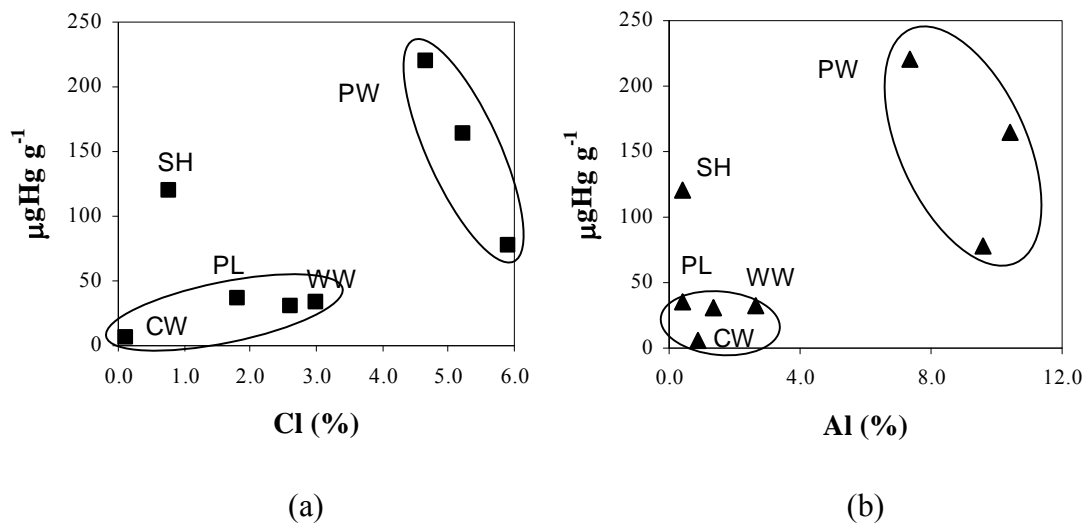


Figure 5.

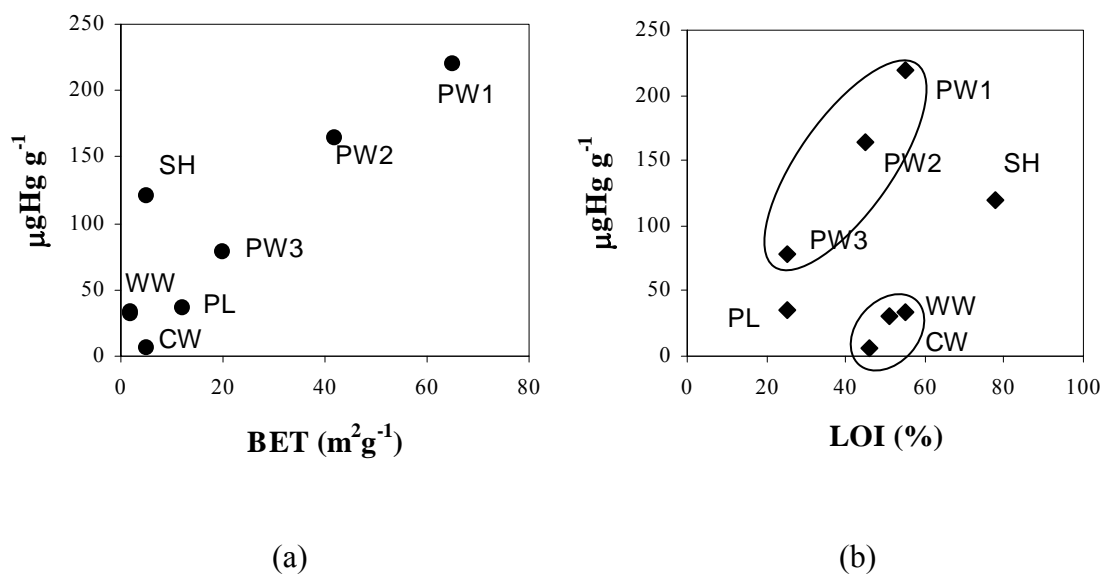


Figure 6.